High-temperature thermodynamics of the Hubbard model: An exact numerical solution*

P. B. Visscher†
Department of Physics and Materials Research Laboratory, University of Illinois, Urbana, Illinois 61801
(Received 22 February 1973)

A new first-principles method for numerically calculating finite-temperature properties of quantum many-body systems is described. It is used to compute the thermodynamic properties and magnetic correlations of the Hubbard model, with negligible error at temperatures near the bandwidth or above. Results for the half-filled band and a simple cubic or one-dimensional lattice confirm the existence of a high-temperature peak in the specific heat which has been associated with a smooth but rapid change in conductivity. Correlations calculated for the non-half-filled band simple cubic Hubbard model suggest condensation, an entirely unexpected phenomenon whose existence is shown (by unrelated methods) in Paper II.

I. INTRODUCTION

A new method is described in this paper for calculating the finite-temperature properties of quantum systems, and applied to the one- and three-dimensional Hubbard[1] models. The Hubbard model is the simplest model of a system of interacting itinerant electrons. Accordingly, it has been the subject of much recent investigation. The present calculation differs from most of this work in that it is exact in a numerical sense; that is, given a choice of the parameters of the model, a temperature (above any singularities), and any desired accuracy, one can calculate all the equilibrium properties of the system to that accuracy. In fact, a computer program has been written which does this (given enough time and memory capacity) for a wide class of models including Hubbard's. Other exact numerical work[2] on the Hubbard model has been done in the one-dimensional case, by exactly solving N atom finite chains and rings and extrapolating to $N=\infty$. The specific heats calculated by Shiba and Pincus[2] (who used $N\leq 6$) for the half-filled band case are confirmed at high temperatures by the present results. More important, the present method can be extended to three dimensions, in which the finite-system extrapolation approach is essentially hopeless (even $2\times 2\times 2$ atoms present a formidable problem). For a half-filled simple cubic model with strong interactions we obtain a smooth high-temperature peak in the specific heat (see, for example, Fig. 6). This extends earlier results[3] (exact only in the limit $t\to 0$) which give such a peak and associate it with a rapid but smooth change in the conductivity. These findings contradict some previous work[4] (based on the Hartree-Fock approximation[5]) which predicted a sharp metal-insulator transition.[6] At lower temperatures we find antiferromagnetic correlations appearing, suggesting the existence of a previously predicted sharp antiferromagnetic transition. For the non-half-filled band, we find positive short-range density-density correlations indicating clustering which suggests a condensation transition. In the following paper[7] it is shown by zero-temperature arguments that a condensation probably occurs, and its implications for the physical applicability of the model are discussed.

In Hubbard's original work on this model, he wrote equations of motion for the Green's functions (as functions of time) and truncated them to obtain a closed system of equations. Our approach differs in that we write differential equations for equal-time expectation values as functions of inverse temperature $\beta=1/kT$ (instead of time). These equations (suitably transformed, as in Sec. II) can then be truncated at any point and integrated to obtain arbitrarily accurate results.[8] Our method is closely related to the well-known technique of high-temperature series expansion, in which expectation values of simple operators are expanded about infinite temperature in a power series in $\beta=1/kT$; this series is easily generated from our equations.

We shall derive our basic differential equations in Sec. II, and briefly describe a computer code for automatically generating and solving them in Sec. III. We give some selected numerical results in Sec. IV, and conclude with Sec. V.

Since the method of Sec. II is quite involved, an effort has been made in Secs. IV and V to make the physical results understandable to the reader who wishes to skip Secs. II and III.

II. DERIVATION OF METHOD

We will use second-quantized notation; $c^{\dagger}_{\vec{R}\sigma}$ and $c_{\vec{R}\sigma}$ create and destroy an electron of spin σ on lattice site $\vec{R}$, and $n_{\vec{R}\sigma}=c^{\dagger}_{\vec{R}\sigma}c_{\vec{R}\sigma}$ is the number operator. The Hubbard Hamiltonian ($\mathcal{H}_{\text{Hub.}}$, for nearest-neighbor hopping, as usual) is

$$\mathcal{H}_{\text{Hub.}}=I\sum_{\vec{R}}n_{\vec{R}\uparrow}n_{\vec{R}\downarrow}-t\sum_{\vec{R},\vec{R}',\sigma}c^{\dagger}_{\vec{R}\sigma}c_{\vec{R}'\sigma}\quad . \tag{1}$$

Here we restrict $\vec{R}$ and $\vec{R}'$ to be nearest neighbors; I is the intra-atomic Coulomb repulsion, and t is

an overlap integral ($t>0$). We will derive our differential equation in the grand canonical ensemble (GCE)[9]; thus we must add a chemical potential term to the Hamiltonian

$$\mathcal{H}_{\mathrm{GCE}} = \mathcal{H}_{\mathrm{Hub.}} + \mu \sum_{\vec{R},\sigma} n_{\vec{R},\sigma} \quad . \tag{2}$$

For notational convenience we will write the Hamiltonian as

$$\mathcal{H}_{\mathrm{GCE}} = \sum_{\alpha} \gamma_{\alpha} \mathcal{H}_{\alpha} \quad , \tag{3}$$

where the $\mathcal{H}_{\alpha}$ are products of $c^{\dagger}$'s and c's (i.e., $\mathcal{H}_{\alpha} = n_{\vec{R}\uparrow} n_{\vec{R}\downarrow}$, $c_{\vec{R}\sigma} c^{\dagger}_{\vec{R}'\sigma}$, or $n_{\vec{R}\sigma}$); the numerical coefficients are γ_{α} (so $\gamma_{\alpha} = I$, t, or μ).

Then the expectation value of an operator A (a product of $c^{\dagger}$'s and c's) is given by

$$\langle A \rangle = \frac{\mathrm{Tr}\, A \exp(-\beta \mathcal{H}_{\mathrm{GCE}})}{\mathrm{Tr} \exp(-\beta \mathcal{H}_{\mathrm{GCE}})} \quad , \tag{4}$$

where Tr indicates a trace over all possible states.

Our differential equation is obtained by simply differentiating Eq. (4) formally[10] with respect[11] to β

$$\frac{d\langle A \rangle}{d\beta} = -\langle A \mathcal{H}_{\mathrm{GCE}} \rangle + \langle A \rangle \langle \mathcal{H}_{\mathrm{GCE}} \rangle \quad . \tag{5}$$

In the limit of an infinite system, both terms on the right-hand side in Eq. (5) are infinite. These divergences must cancel, as we can show explicitly by substituting Eqs. (3) into (5) and rearranging terms;

$$\frac{d\langle A \rangle}{d\beta} = -\sum_{\alpha} \gamma_{\alpha} \left(\langle A \mathcal{H}_{\alpha} \rangle - \langle A \rangle \langle \mathcal{H}_{\alpha} \rangle \right) \quad . \tag{6}$$

In the absence of long-range correlations (i.e., at temperatures above any critical temperatures which may exist) the quantity in parentheses in Eq. (6) goes to zero rapidly as $\mathcal{H}_{\alpha}$ becomes spacially separated from A; it is, in fact, a measure of the correlation between $\mathcal{H}_{\alpha}$ and A.

We have thus shown the sum in Eq. (6) to be convergent. It gives us a system of coupled differential equations (one for each A). For purposes of actual calculation, Eq. (6) shares a difficulty with all such many-particle equations of motion: the derivative of an N-particle operator involves $(N+1)$- and $(N+2)$-particle operators. (A is an N particle, or Nth order operator if it has N $c^{\dagger}$'s and N c's.) The solution adopted by Hubbard in his original work[1] was to write high-order operators as products of lower-order ones. We shall do this in a more systematic way by decomposing the expectation values $\langle A \rangle$ into cumulants.[12] The cumulant associated with A will be denoted by (A). The cumulant (A) may be written in terms of $\langle A \rangle$ and lower-order expectation values, but it is more convenient to define it inductively on N, the order of the cumulant. The one-particle cumulants are defined by $(A) = \langle A \rangle$, i.e.,

$$(c_i^{\dagger} c_j) = \langle c_i^{\dagger} c_j \rangle \tag{7}$$

(we have replaced $\vec{R}\sigma$ by a composite index). If the cumulants of order less than N are known, a cumulant (A) of order N may be obtained from

$$\langle A \rangle = \sum_{B_1 \cdots B_n = A} (B_1) \times \cdots \times (B_n) \quad , \tag{8}$$

where the sum is over all distinct factorizations $B_1 \times B_2 \times \cdots \times B_n$ of A.

In Eq. (8), as well as all our later sums over factorizations, certain things are implicit: (i) All operators are in normal form ($c^{\dagger}$ precedes c); (ii) noncommutation of operators is ignored, except that if an odd permutation of the $c^{\dagger}$'s and c's is necessary to bring A into the form $B_1 \cdots B_n$, a minus sign is inserted; (iii) in enumerating distinct factorizations, all $c^{\dagger}$'s and c's are regarded as distinct (even if they really aren't). In the present case, (iii) is irrelevant [if A has two identical operators, $\langle A \rangle$ and (A) vanish] but it will become relevant later [Eq. (10)].

As an example of Eq. (8), we write the equation defining the two-particle cumulants

$$\langle c_i^{\dagger} c_j^{\dagger} c_k c_l \rangle = (c_i^{\dagger} c_j^{\dagger} c_k c_l) + (c_i^{\dagger} c_l)(c_j^{\dagger} c_k) - (c_i^{\dagger} c_k)(c_j^{\dagger} c_l) \quad . \tag{9}$$

Equation (9) shows that the two-particle cumulant is actually the difference between an expectation value and its Hartree-Fock decomposition. Thus if the Hartree-Fock approximation[13] is fairly good, the information contained in the one- and two-particle expectation values is mostly recoverable from the one-particle cumulants via Eq. (8). Generalizing this, it seems likely (and can be verified numerically) that the cumulants provide a much more economical way of representing the state of the system than do the expectation values. So, although our purpose in introducing cumulants was just to factor $\langle A \mathcal{H}_{\alpha} \rangle$ in Eq. (6), we are better off eliminating the bare expectation values entirely and writing a differential equation just for the cumulants.

We will do this at first by assuming the $c^{\dagger}$'s and c's of A and $\mathcal{H}_{\alpha}$ in Eq. (6) anticommute, even those referring to the same orbital. (This simplifies the problem because $A\mathcal{H}_{\alpha}$ can then be brought to normal form without introducing extra terms.) Our procedure will be to make a guess at $d(A)/d\beta$, and verify it by induction on the order of A. The guess is

$$\frac{d(A)}{d\beta} = -\sum_{\alpha} \gamma_{\alpha} \sum_{\substack{B_1 \cdots B_n = A\mathcal{H}_{\alpha} \\ (\text{all } B_i \text{ overlap } \mathcal{H}_{\alpha})}} (B_1) \cdots (B_n) \quad , \tag{10}$$

where the sum is over all factorizations of $A\mathcal{H}_{\alpha}$

into $B_1 \times \cdots \times B_n$, subject to the condition that each B_i must overlap $\mathcal{K}_\alpha$ (i.e., share at least one $c^\dagger$ or c with $\mathcal{K}_\alpha$.) To verify our guess (10), we substitute (8) into (6).

$$\sum_{B_1 \cdots B_n = A} \sum_{j=1}^{n} (B_1) \cdots \frac{d(B_j)}{d\beta} \cdots (B_n)$$

$$= -\sum_\alpha \gamma_\alpha \Bigg(\sum_{B_1 \cdots B_n = A\mathcal{K}_\alpha} (B_1) \cdots (B_n) - \sum_{E_1 \cdots E_n = A} (E_1) \cdots (E_n) \sum_{D_1 \cdots D_p = \mathcal{K}_\alpha} (D_1) \cdots (D_p) \Bigg) . \tag{11}$$

Note that the second sum on the right-hand side of Eq. (11) cancels part of the first, namely, those terms in which no B_i overlaps both A and $\mathcal{K}_\alpha$. Using this fact, and substituting (10) for the derivative on the left, we get

$$-\sum_\alpha \gamma_\alpha \sum_{B_1 \cdots B_n = A} \sum_{j=1}^{n} (B_1) \cdots \times \Bigg(\sum_{\substack{D_1 \cdots D_p = B_j \mathcal{K}_\alpha \\ \text{(each } D_i \text{ overlaps } \mathcal{K}_\alpha)}} (D_1) \cdots (D_p) \Bigg) \cdots (B_n)$$

$$= -\sum_\alpha \gamma_\alpha \sum_{\substack{E_1 \cdots E_n = A\mathcal{K}_\alpha \\ \text{(some } E_i \text{ overlaps } A \text{ and } \mathcal{K}_\alpha)}} (E_1) \cdots (E_n) . \tag{12}$$

Recall that Eq. (11) is true, but (12) depends on (10) and has not yet been proved. But if we can demonstrate (12) independently of (10), we will have proved (10) by induction on the order of A! For (10) is trivially true for all A's of order zero (there are none.) And assuming it for all lower-order cumulants than (A), we may prove it for (A) as follows: all the cumulants (B_j) whose derivatives appear in (11) are of lower order except one, namely, (A) itself, from the trivial factorization with $n=1$. So we may use (10) for these others, giving us a true equation, say (12′), identical to (12) except that one term on the left-hand side of (12′) still is the left-hand side of (10), whereas the right side of (10) has been substituted in (12). Since (12′) and (12) are both true, the left and right sides of (10) are equal, i.e., (10) is true of (A).

So now we need only prove Eq. (12). This is done simply by observing that the same terms appear on both sides. For each $(E_1) \cdots (E_n)$ on the right side, the E's which do not overlap $\mathcal{K}_\alpha$ become B's, and those which do become D's.

We have been assuming the $c^\dagger$'s and c's anticommute, to avoid unnecessary confusion. We will now go back and take account of the canonical relation

$$c_i c_i^\dagger = 1 - c_i^\dagger c_i . \tag{13}$$

In going from Eq. (6) to (11), we must be more careful in expressing $\langle A\mathcal{K}_\alpha \rangle$ in terms of cumulants; it is not in normal form. If we write out $A\mathcal{K}_\alpha$, collect the noncommuting pairs $c_i c_i^\dagger$ (where c_i is from A and $c_i^\dagger$ from $\mathcal{K}_\alpha$) and use (13) for each of them, we see that

$$A\mathcal{K}_\alpha = \sum_F N\left\{\frac{A\mathcal{K}_\alpha}{F}\right\} , \tag{14}$$

where N indicates normal form and F is a product of noncommuting pairs. By $A\mathcal{K}_\alpha/F$, we mean $A\mathcal{K}_\alpha$ with F removed (and a minus sign, if removal requires an odd permutation). The sum includes the trivial F with zero pairs; this gives a term $N\{A\mathcal{K}_\alpha\}$. Equation (14) is a version of Wick's theorem.

Now we can correct Eq. (11); instead of summing over factorizations of $A\mathcal{K}_\alpha$, we sum over factorizations of $A\mathcal{K}_\alpha/F$ for all possible F. Then the proof of (10) goes through as before, if we replace (10) by

$$\frac{d(A)}{d\beta} = -\sum_\alpha \gamma_\alpha \sum_{\substack{B_1 \cdots B_n F = A\mathcal{K}_\alpha \\ \text{(each } B_i \text{ overlaps } \mathcal{K}_\alpha)}} (B_1) \cdots (B_n) , \tag{15}$$

where the inner sum is over all factorizations of $A\mathcal{K}_\alpha$ into $B_1 \cdots B_n F$. F is a product of zero or more pairs $c_i c_i^\dagger$ with c_i from A, $c_i^\dagger$ from $\mathcal{K}_\alpha$. We give explicitly a few terms of Eq. (15) in Table III. These can easily be checked by hand.

Equation (15) is the basis for our calculation. We wish to integrate this differential equation from $\beta = 0$ to obtain finite-temperature values for the cumulants (A). Because of translational symmetry, for each (A) there are infinitely many others with the same value; clearly we must exploit this symmetry. To make our method efficient enough to be of much use we must also exploit the other symmetries of the system. These include space rotation, spin rotation, and time reversal. The space rotation group is the 48-element octahedral group O_h (Shoenflies notation). Since we only need spin rotations to interchange $c_{R\uparrow}^\dagger$ with $c_{R\downarrow}^\dagger$, our spin-rotation group need have only two elements, the identity e and a rotation ω (by π about the x axis, for example) which reverses the z component of the spin. Instead of time reversal it is more

TABLE I. Inequivalent operators in the Hubbard Hamiltonian [Eq. (3)], with integer labels. All operators are in normal form, though we sometimes write A for $N\{A\}$, for convenience.

Integer label	Operator $\mathcal{K}_{\bar{\alpha}}$	Coefficient $\gamma_{\bar{\alpha}}$
1	$n_{(000)\uparrow}$	μ
2	$c_{(000)\uparrow}\, c^\dagger_{(100)\uparrow}$	t
3	$n_{(000)\uparrow}\, n_{(000)\downarrow}$	I

TABLE II. Simple cumulants (in our arbitrarily chosen standard form) with their labels. We again write $\bar{A}$ for $N\{\bar{A}\}$.

Integer label	Operator $\bar{A}$
1	$n_{(000)\uparrow}$
2	$c_{(000)\uparrow}$, $c^{\dagger}_{(100)\uparrow}$
3	$n_{(000)\uparrow}$, $n_{(000)\downarrow}$
4	$n_{(000)\uparrow}$, $c^{\dagger}_{(000)\downarrow}$, $c_{(001)\downarrow}$
5	$c_{(000)\uparrow}$, $c^{\dagger}_{(002)\uparrow}$
6	$c^{\dagger}_{(000)\uparrow}$, $c_{(011)\uparrow}$

convenient to simply use the Hermitian conjugation operation K. Because the cumulants happen to be real, they are invariant under K, and the fact that K is antilinear rather than linear has no effect. The total invariance group of the system is the product of these four groups (translation, space and spin rotation, and Hermitian conjugation). We will denote it by G.

The set of products A of $c^{\dagger}$'s and c's (in normal form) is partitioned into equivalence classes by G. We arbitrarily choose one member $\bar{A}$ of each class, and concern ourselves only with calculating the cumulant $(\bar{A})$. For any other member A, we have $A = g\bar{A}$ with $g \in G$, so clearly $(A) = (\bar{A})$. The terms of the Hamiltonian (3) are similarly partitioned; we denote the distinguished member of a class by $\mathcal{H}_{\bar{\alpha}}$. The $\mathcal{H}_{\bar{\alpha}}$'s are listed in Table I, and some of the $\bar{A}$'s in Table II.

We now describe a finite procedure for solving (15) numerically. We attempt in this section only to convey a general understanding of how this is possible; a precise description is left for the Appendix.

We must somehow decide how to truncate the system of equations; that is, which $(\bar{A})$'s to calculate and which to ignore. The feature of (15) which makes it so attractive for automatic computation is that it makes this decision for us; this is unique among equation-of-motion truncation schemes. Initially (at $\beta = 0$), it can be shown that the only nonzero cumulants are $(n_{\vec{R}\sigma})$, i.e., the equivalence class of $\bar{A} = n_{\vec{0}\uparrow}$. So we have only one nonzero $(\bar{A})$, with the numerical value ρ, the density per orbital. Thus in Eq. (15) the only nonzero terms on the right-hand side are those in which all the B's are equivalent to $n_{\vec{0}\uparrow}$. Clearly (because of the crucial restriction that B_i overlap $\mathcal{H}_{\alpha}$), there are a finite number (in fact, exactly nine, four of which have been included in Table III) of inequivalent ways of arranging the B_i's and F on the $\mathcal{H}_{\alpha}$'s, and hence only a finite number (exactly three) of inequivalent (A)'s whose derivatives are nonzero. We use these nonzero derivatives computed from Eq. (15) to increment the cumulants

$$(\bar{A})_{\beta+\Delta\beta} = (\bar{A})_{\beta} + \Delta\beta \left(\frac{d(\bar{A})}{d\beta}\right) , \tag{16}$$

where $\beta = 0$ for the first iteration, and $\Delta\beta$ is a small constant increment. After this first iteration the number of nonzero $(\bar{A})$'s is still finite (three). Clearly, this remains true in later iterations; if a finite number of $(\bar{A})$'s are nonzero, there are a finite number of products $\gamma_{\bar{\alpha}}(\bar{B}_1)\cdots(\bar{B}_n)$ (in the more precise notation of the Appendix, a finite number of P's) contributing to Eq. (15). (This finiteness depends on the fact that n is bounded.[14]) And each such set of $\bar{B}$'s can be arranged around the $\mathcal{H}_{\bar{\alpha}}$'s in a finite number of inequivalent ways, giving nonzero derivatives for only a finite number of $(\bar{A})$'s. We therefore have a finite algorithm for solving Eq. (15): we pick a $\Delta\beta$ by which to increment β from $\beta = 0$, and at each iteration we enlarge our list of $(\bar{A})$'s to include all those generated by (15) from our previous list. By using a small enough $\Delta\beta$, we can compute the finite-temperature cumulants to arbitrary accuracy.

This algorithm rapidly accumulates a large number of cumulants with extremely small numerical values. To avoid this, instead of considering all products of cumulants, we use only those which (at the particular β we have reached) exceed some small positive number δ;

$$\left| \gamma_{\alpha}(B_1)\cdots(B_n) \right| > \delta \quad . \tag{17}$$

This eliminates unnecessary calculation, while ensuring that no important term is thrown away. It is clear that this modified algorithm is still exact, in the sense that we can achieve arbitrary accuracy (at a given β) by choosing $\Delta\beta$ and δ small enough.

TABLE III. Selected terms in the differential equation (15) [or (A9)], for the simple cubic lattice. Integer labels for $\mathcal{H}_{\bar{\alpha}}$ are from Table I, labels for $\bar{B}_i$ and $\bar{A}$ from Table II. The tabulated coefficient is the coefficient of $-\gamma_{\bar{\alpha}}(\bar{B}_1)\cdots(\bar{B}_n)$ in $d(\bar{A})/d\beta$ (i.e., $f_a f_s$ in the notation of the Appendix).

$\mathcal{H}_{\bar{\alpha}}$ label	$\bar{B}_i$ labels	$\bar{A}$ label	Coefficient
3	1	None	
1	1	1	1
2	1	2	1
3	1,1,1	1	−1
		3	−2
2	3	4	−1
2	2	1	6
		5	−1
		6	2
1	3,1	3	−4

III. DESCRIPTION OF MACHINE CALCULATION

To test the method described in Sec. II and the Appendix, a computer program was written. It was not our objective to push the method to obtain the highest possible accuracy or lowest temperatures for any of the particular cases considered below, but rather to see how promising the method seems in a wide variety of cases. The program was therefore designed to be as general as possible. Even the Hubbard model is not built in; the Hamiltonian need only have the form (3), on a cubic lattice with one s orbital per site. The program is converted for the one-dimensional chain by changing three FORTRAN lines. As a result of this generality, the program is not very efficient for any of the models, especially in one dimension. Also, for some choices of parameters there is much cancellation in (15), and determining which terms to include by a different criterion than (17) would speed convergence. It should therefore be kept in mind, in looking at the numerical results for special cases below, that each of them is almost certainly capable of substantial improvement with a small investment of effort.

Because of the nature of the algorithm, the program must be able to take an arbitrarily complicated operator A and put it in a unique standard form $\overline{A}$. It must ensure that each inequivalent relative geometric arrangement of $\mathcal{K}_\alpha$, F, $B_1 \cdots B_n$ (each $\overline{C}$ in the notation of the Appendix) is considered exactly once (this is especially difficult if some B_i's are equivalent). Proper treatment of the symmetry requires algorithms for various group-theoretic manipulations of arbitrary subgroups of the group G. Thus the program is necessarily rather complex, and cannot be described here except in general outline.

The inputs to the program are the Hamiltonian operators $\mathcal{K}_{\overline{\alpha}}$ (Table I), their coefficients $\gamma_{\overline{\alpha}}$ (i.e., t and I; μ' is determined as in Ref. 10), the density ρ, and the error tolerance δ [Eq. (17)].[15] The program then generates the terms in (15) as required. It terminates when it fills the memory space provided for storing information (like that in Table III) specifying these terms, say N_t words (an average of three words per term). The value of β at which this occurs will be denoted by β_t. (In practice, the system of equations defined by these terms is then integrated again from $\beta = 0$ to obtain better accuracy; this integration need not stop at β_t.) This particular truncation of Eq. (15) is uniquely determined by δ and N_t (and, of course, t, I, and ρ). We will generally specify it by δ, N_t, and β_t to give an idea of the size of the ignored terms ($\leq \delta$), the interval in $\beta = 1/kT$ over which they do not exceed δ(0 to β_t), and the required data storage ($\leq 2N_t$ words, counting storage of the cumulants themselves as well as the differential equation). The computing time is roughly proportional to N_t. The longest calculation we have done ($N_t = 5000$) takes about 14 min on the XDS Sigma 5, a relatively slow computer, and costs about \$11.

A number of checks have been made of the accuracy of the program. During debugging, several hundred machine-generated terms in Eq. (15) were checked by hand, most of them after the last error was corrected. In addition, several tests have been made on the final program. The Hubbard model can be solved analytically in two limiting cases, the atomic limit ($t = 0$) and the noninteracting limit ($I = 0$). In the atomic limit, the only nonzero cumulants are $\langle n_\uparrow \rangle$ and $\langle n_\uparrow n_\downarrow \rangle$, and (15) is a closed system of equations. The program was tested for $\rho = \frac{1}{2}$ (half-filled band) and reproduced the exact solution (Fig. 1).

The noninteracting limit is less trivial. Our method, based on local operators, is not naturally suited for describing band wave functions; thus this limit provides a test of the convergence of the method, as well as the correctness of the program. The exact specific heat in one dimension is given by Shiba and Pincus.[2] We calculated it out to $\beta = 4.2$ (for $t = 1.0$, using $\delta = 2.5 \times 10^{-7}$, $N_t = 499$, $\beta_t = 2.4$) reproducing their result exactly to within the width of their curve. In three dimensions convergence is naturally not so rapid, but we are still able to reproduce the specific-heat peak exactly (Fig. 2). This calculation used $N_t = 5000$ (about 1700 terms) and 103 cumulants $[\langle c_{\vec{0}\uparrow} c_{\vec{R}\uparrow} \rangle$ for 103 inequivalent $\vec{R}$'s, roughly filling a sphere of radius 9 lattice spacings]. At very low temperatures more distant neighbors become important, causing deviation from the exact result.

The program cannot be checked outside these two limits for the Hubbard model, because no accurate calculation exists. However, the Ising Hamiltonian can also be cast into the form (3); from the resulting coupled equations (15) high-temperature series may be derived for all the cumulants. The series for all the spin-spin correlations were obtained to third order, and agree

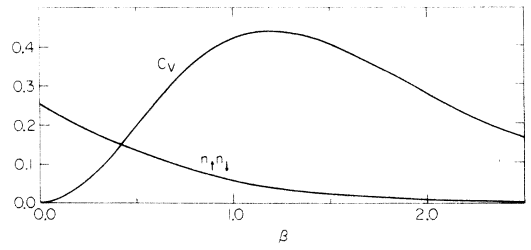

FIG. 1. Specific heat C_V and fraction of doubly occupied sites $\langle n_\uparrow n_\downarrow \rangle$, for the atomic limit (independent of dimensionality) using $\rho = \frac{1}{2}$, $t = 0$, and $I = 4$. The calculated curves coincide with the exact results, $C_V = [x/(1+e^x)]^2 e^x$ and $\langle n_\uparrow n_\downarrow \rangle = (\frac{1}{2})(1+e^x)^{-1}$, where $x = \frac{1}{2}\beta I$.

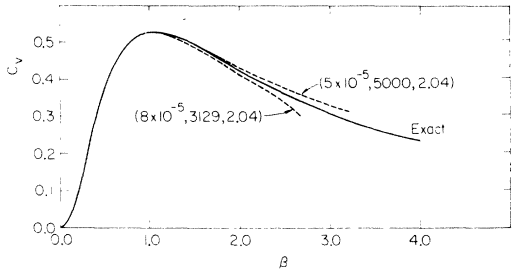

FIG. 2. Specific heat of the simple cubic noninteracting case ($\rho=\frac{1}{2}$, $t=1$, $I=0$). Our results (dashed curves labeled by δ, N_t, β_t) are plotted with the exact result (solid curve obtained by integrating the known density of states; the author is indebted to B. Yang for a program to do this).

exactly with known results[16] for the simple cubic lattice.

A consistency check can be made by noting that (5) could have been written with $\langle \mathcal{H}A\rangle$ replacing $\langle A\mathcal{H}\rangle$. This has the effect in (15) of conjugating F (i.e., $c^\dagger$ now comes from A, c from $\mathcal{H}_\alpha$). The new coupled equations for the cumulants then look quite different from the old ones (if we allow the standard forms $\overline{A}$ to remain the same). For example, the sixth line of Table III disappears. This variation was tried for the case shown below in Fig. 4(c); the results were the same to within the convergence error. This is strong evidence for the correctness of the program, since it is unlikely an error would affect the two calculations the same way.

IV. NUMERICAL RESULTS

In order to compare the results of our method with the only other exact results available, we ran our program for some of the cases considered by Shiba and Pincus.[2] These involve a one-dimensional infinite chain with one electron per atom (half-filled band, $\rho=\frac{1}{2}$) whose properties Shiba and Pincus tried to extrapolate from exact calculations of finite chains. The problem is determined by one parameter t/I. Shiba and Pincus distinguish two cases: weak interaction ($I<4t$ = bandwidth) and strong interaction ($I\gtrsim 4t$). In the former case their specific heat has one peak, and is not qualitatively different from the noninteracting case. Our results for the weakly interacting ($t/I=2$) infinite chain are shown in Fig. 3(a), for three different values of the error cutoff δ. The convergence is essentially complete on the high-temperature side of the peak. We replot our best result [i.e., $\delta=10^{-4}$, with conservative error bars based on the apparent rate of convergence of Fig. 3(a)] in Fig. 3(b) along with Shiba and Pincus's finite-chain results. It is apparent that the present method converges much more rapidly at high temperatures ($\beta\lesssim 1.3$); though it is not hard to believe that the finite-chain results converge to the exact curve, it cannot be well determined by extrapolating them. The specific heat for the simple cubic lattice, using the same parameters, is shown in Fig. 3(c). In spite of the much greater complication of the 3-D calculation, we still resolve the peak well.

For strong interactions the specific heat no longer resembles the noninteracting result. For $t/I\ll 1$, simple perturbation theory shows that at temperatures $kT\ll I$ the Hubbard model behaves as a Heisenberg model with exchange parameter

$$J=2t^2/I \quad . \tag{18}$$

From known results[17] for the Heisenberg model, we expect in one dimension a peak in the specific heat due to the appearance of antiferromagnetic or-

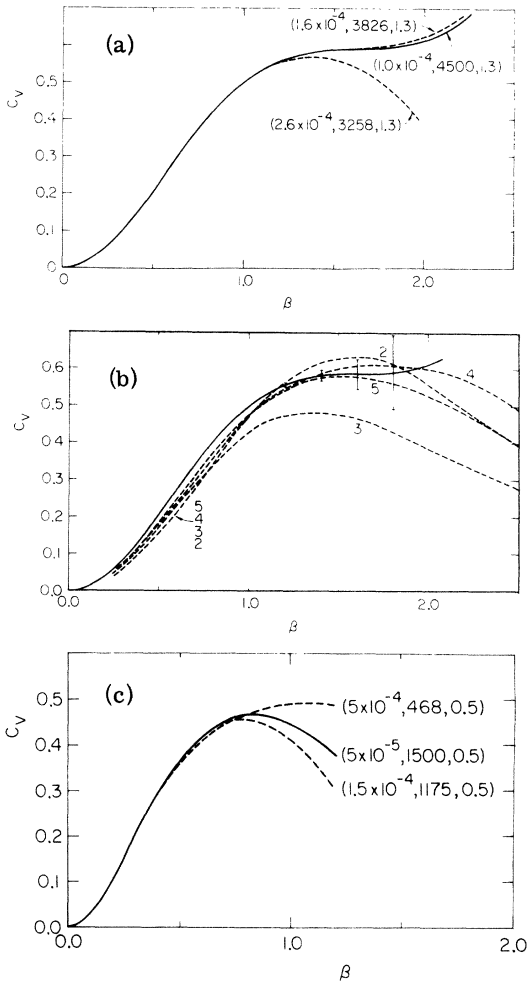

FIG. 3. Specific heat of the weakly interacting half-filled Hubbard model ($\rho=\frac{1}{2}$, $t=1$, $I=\frac{1}{2}$. (a) one-dimensional, our results labeled by (δ, N_t, β_t). (b) Our result (solid line) with Shiba and Pincus's results for 2, 3, 4, and 5 atom chains. (c) Our three-dimensional result.

dering at about $kT \approx 2t^2/I$. This peak was found by the workers of Ref. 2 for finite chains. Because of the relatively long range of the ordering, this peak is not easily accessible by our present method (although we do verify the appearance of short-range antiferromagnetic correlations).

Shiba and Pincus also report a higher-temperature peak which they associate with a metal-insulator transition (but see Ref. 6). This peak is well resolved by our calculation.[18] Our results for the strongly interacting ($t/I = \frac{1}{4}$) infinite chain are shown in Fig. 4(a). Our best result is compared to Shiba and Pincus's finite-chain results in Fig. 4(b). As in Fig. 3(b), there is good general agreement.

The physical interpretation of this high-temperature peak was given by Shiba and Pincus.[2] It is most easily seen in the atomic limit, shown in Fig. 1. The peak here is due to the freezing out of doubly occupied sites when $kT \ll I$; at low temperatures

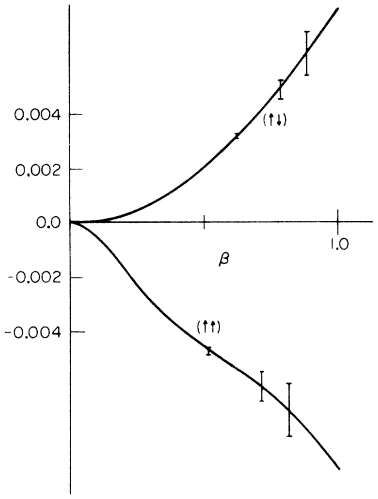

FIG. 5. Magnetic correlations for the case of Fig. 4(c). Curve labeled (↑↓) is $\langle n_{(000)\uparrow} n_{(001)\downarrow}\rangle - \langle n\rangle^2$, and (↑↑) is $\langle n_{(000)\uparrow} n_{(001)\uparrow}\rangle - \langle n\rangle^2$. Indicated errors are estimated from rate of convergence.

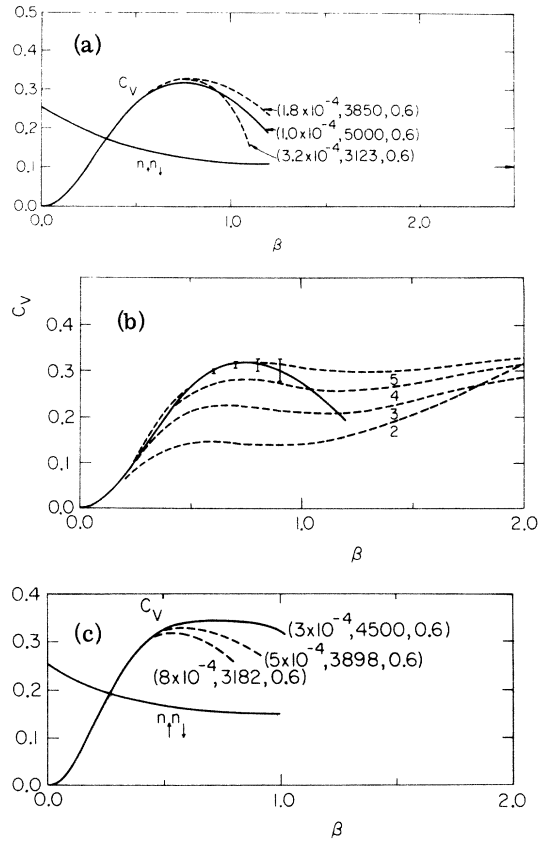

FIG. 4. Specific heat for fairly strong interaction ($\rho = \frac{1}{2}$, $t = 1$, $I = 4$). (a) Our one-dimensional results; curves labeled by (δ, N_t, β_t). Fraction $\langle n_\uparrow n_\downarrow\rangle$ of doubly occupied sites also given; arrow at right indicates exact $\beta = \infty$ value. (b) Our result (solid line) with 2, 3, 4, and 5 atom chain results (Shiba and Pincus). (c) three-dimensional result; $\langle n_\uparrow n_\downarrow\rangle$ also given.

only one electron per site is allowed (i.e., we have "local moments"[2]). Figure 1 also shows how the probability of double occupancy (i.e., $\langle n_{\delta\uparrow} n_{\delta\downarrow}\rangle$) decreases. This freezing out causes a rapid decline in conductivity because the current carriers are extra electrons (doubly occupied sites) and holes (empty sites). In the atomic limit there is of course no conductivity, but for small nonzero t the conductivity is proportional to t^2 and has been explicitly calculated in this limit by Bari and Kaplan[3] who confirm the rapid change in conductivity near the specific-heat peak.

To show that the specific-heat peaks for the interacting systems in Fig. 4 are attributable to this same mechanism, we include $\langle n_\uparrow n_\downarrow\rangle$ in Figs. 4(a) and 4(c).[19] We see that the peaks correspond to a rapid decrease in $\langle n_\uparrow n_\downarrow\rangle$, but that it does not disappear entirely, as it does in the atomic limit. This is because for finite t/I, $\langle n_\uparrow n_\downarrow\rangle$ does not vanish even at zero temperature; some double occupancy is allowed because the kinetic energy is thereby decreased. In one dimension, the zero-temperature value of $\langle n_\uparrow n_\downarrow\rangle$ can be obtained[2] from the exact solution of Lieb and Wu.[20] It is shown as an arrow in Fig. 4(a). It can be seen that the freezing-out is essentially complete[21] at $\beta \approx 1.2$.

Our present method does not explicitly demonstrate the rapid drop in conductivity associated with this freezing-out (we do not obtain any nonequilibrium properties; this would be an interesting subject for future investigation[8]). But Bari and Kaplan's conductivity calculation[3] (which is correct as $t \to 0$ for fixed nonzero kT and I) indicates that such a drop occurs for small t/I.

Figure 4(c) gives the three-dimensional result

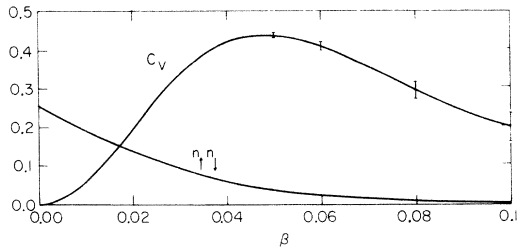

FIG. 6. Specific heat and $\langle n_\uparrow n_\downarrow \rangle$ for very strong interaction ($\rho = \frac{1}{2}$, $t = 1$, $I = 100$).

for the same parameters used in Figs. 4(a) and 4(b). The specific-heat peak is very broad; indeed it is not clear if it turns downward at all. We believe that the high-temperature peak is beginning to merge into the lower-temperature antiferromagnetic structure. The Heisenberg-model analogy [Eq. (18)] and series results for the Heisenberg model[22] suggest we may expect a transition around $kT \approx 1.90J \approx 0.95$, or $\beta \approx 1.05$. Though it is not clear whether $t/I = \frac{1}{4}$ is small enough to actually induce a transition, we observe an antiferromagnetic tendency in the nearest-neighbor magnetic correlations (Fig. 5; we plot these rather than the susceptibility because the latter is dominated at these temperatures by intra-atomic effects).

To see the high-temperature peak in C_V (and the associated freezing-out of doubly occupied sites) uncluttered by magnetic effects, we must consider very strong interactions ($t/I \ll 1$), for which the antiferromagnetic structure recedes to very low temperature ($kT \sim 4t^2/I$) with respect to the high-temperature peak, which remains at $kT \sim 0.2I$. The specific heat C_V and $\langle n_\uparrow n_\downarrow \rangle$ for $t/I = \frac{1}{100}$ are shown in Fig. 6. C_V resembles the atomic limit at high temperatures, but exceeds it at low temperatures with the gradual appearance of antiferfomagnetic correlations.

Our most surprising results were obtained for the non-half-filled band. To test Nagaoka's prediction[23] of a ferromagnetic ground state for densities near the half-filled band and small t/I, we calculated the specific-heat and nearest-neighbor correlations for $\rho = 0.35$ (i.e., 0.7 e/atom) and $t/I = \frac{1}{25}$. Figure 7 shows the results. The correlations are antiferromagnetic at high temperatures; as we lower the temperature the parallel-spin correlation curves upward and becomes positive, as we expect (in our grand canonical ensemble) if the ground state is to be ferromagnetic. But the antiparallel-spin correlation does not become negative, as it should. The fact that we have *both* correlations positive gives us a net density-density correlation; that is, a clustering effect. This suggests the intriguing possibility of a condensation transition at low temperatures. In fact we find (Paper II[7]) by arguments quite independent of the above numerical results, that for some choices of parameters condensation probably occurs. The zero-temperature state consists of two phases of different densities, an antiferromagnetic phase (density $\rho = \frac{1}{2}$) and a ferromagnetic phase of lower density.

We can use the zero-temperature results to give a heuristic explanation of our high-temperature curves (Fig. 7). The first peak in C_V [Fig. 7(a)] reflects the freezing-out of doubly occupied sites (just as for the half-filled band, but now the holes do not freeze out, so there is no sharp conductivity drop). In general, we expect at high temperatures the formation of small clusters resembling the low-temperature phases; in this case ferromagnetic (F) and antiferromagnetic (AF) clusters. The rise in C_V at the right of Fig. 7(a) is due to the binding energy of these clusters. Since the F clusters contribute mainly to the parallel-spin correlations, (and AF to antiparallel), we can explain Fig. 7(b) by mixing them in the proper proportions. Let us assume the clusters occupy 6% of the volume (73% F, 27% AF) and the other 94% is uncorrelated. Since the AF clusters have density $\rho = \frac{1}{2}$, the F clusters must have $\rho = 0.295$. The antiparallel and parallel correlations come out to be 0.000 75 and 0.000 25 respectively. These fit quite nicely onto Fig. 7(b) at about $\beta = 0.34$; at lower temperatures the cluster volume must increase, and there must be proportionately more

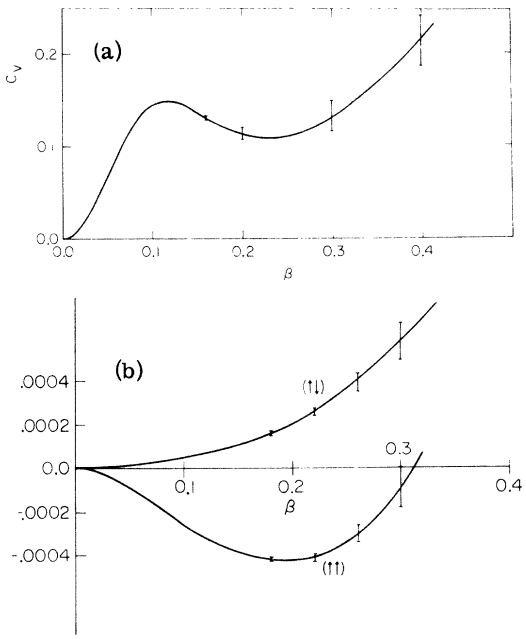

FIG. 7. Non-half-filled band ($\rho = 0.35$, $t = 1$, $I = 25$). (a) Specific heat. (b) Nearest-neighbor correlations, defined as in Fig. 5.

F clusters. It should be noted that this explanation does not depend on the specific parameters used in Fig. 7 giving a system with a two-phase equilibrium at zero temperature; in fact the phase diagram[7] still indicates it to be purely ferromagnetic. At high temperature ($kT \gg t^2/I$) the energies of the ferromagnetic and antiferromagnetic states are indistinguishable, so we expect clusters of each. Though it is important not to take arguments involving these (basically ill-defined) clusters too literally, the intuitive picture they provide of the behavior of the system may be essentially correct.

V. CONCLUSION

We have shown that the differential-equation method derived in Sec. II can produce nontrivial information about problems which were heretofore accessible only by approximate methods of unknown accuracy.

The results so far obtained show that the conductivity drop in the half-filled three-dimensional (simple cubic) Hubbard model is gradual rather than sharp, and that antiferromagnetic correlations exist at high temperatures, supporting previous speculation that the ground state is antiferromagnetic.

At densities other than the half-filled band, we find correlations suggesting condensation into a two-phase system. This prediction is supported by independent examination of the zero-temperature state.[7]

We wish to emphasize the great flexibility of the computational approach used in this calculation, namely that of generating, as well as solving, the equations automatically. Although development of the necessary combinatorial and group-theoretical algorithms required a large initial investment of effort, their generality allows rather fundamental changes to be made in the method with very minor changes in the computer code. For example, for some ranges of parameters the algorithm would converge much more rapidly with a different factorization rule from (8) (e.g., allowing no factorization to separate two operators on the same site). Equations (15) then become completely different, and if we were computing them by hand we would have to start all over. Using the present program, on the other hand, we need only change a few lines.

The principal limitation of our present method is its inability to deal with long-range correlations; work is in progress toward handling these more efficiently.

ACKNOWLEDGMENTS

I would like to thank Leo Falicov for valuable early advice, Bunli Yang for frequent useful conversations and encouragement, and Michael Wortis for many helpful discussions.

APPENDIX

In this Appendix we give a precise description of the algorithm (described in general terms in Sec. II) for integrating the basic equation (15). We first categorize the factorizations on the right-hand side according to the equivalence classes of $\mathcal{K}_\alpha$ and the B_i's. Each category may be labeled by an $(n+1)$-tuple P

$$P = (\mathcal{K}_{\bar{\alpha}},\ \bar{B}_1,\ \cdots \bar{B}_n) \quad , \tag{A1}$$

where we require $\bar{B}_1 \le \bar{B}_2 \le \cdots \le \bar{B}_n$ in some arbitrary ordering, for uniqueness. We can clearly take into account only a finite number of P's; we choose those satisfying (17). Given such a category P, we would like a set of rules for generating all the contributions it makes to the derivatives $d(\bar{A})/d\beta$ in (15). The standard forms in (A1) may be moved around arbitrarily on the lattice (and F chosen in various ways) resulting in many different configurations. We denote a representative configuration by C, defined formally by the $(n+2)$-tuple

$$C = (\mathcal{K}_\alpha,\ F,\ B_1,\ \cdots B_n) \quad . \tag{A2}$$

Here $\mathcal{K}_\alpha = g\mathcal{K}_{\bar{\alpha}}$, $B_i = g_i \bar{B}_i$ for g, $g_i \in G$. To make C unique, we require $B_1 \le B_2 \le \cdots B_n$ in our arbitrary ordering. Clearly C determines the A in Eq. (15) uniquely. Because of rule (iii) listed after Eq. (8), the configuration C may correspond to more than one factorization in (15); if B_i and B_j share an operator $c_k^\dagger$, C does not determine which of the two $c_k^\dagger$'s is assigned to $\mathcal{K}_\alpha$ and which to A. When we convert (15) to a sum over C's, we must sum explicitly over these distinct assignments. We shall also write explicitly the sign of the permutation mentioned in rule (ii), which turns $B_1 \cdots B_n F$ into $A\mathcal{K}_\alpha$. Because this depends on the distinct assignment, we denote it by $\sigma_{\text{d.a.}}$ Equation (15) becomes

$$\frac{d(A)}{d\beta} = -\sum_{C:B_1\cdots B_nF = A\mathcal{K}_\alpha\ (\text{each } B_i \text{ overlaps } \mathcal{K}_\alpha)} \times \sum_{\text{d.a.(each } B_i \text{ overlaps } \mathcal{K}_\alpha)} \delta_{\text{d.a.}}\gamma_\alpha(B_1)\cdots(B_n) \quad . \tag{A3}$$

Here C is as in Eq. (A2). Satisfaction of the overlap condition in the sum over C (where we have not specified which $c_k^\dagger$ is assigned to $\mathcal{K}_\alpha$, hence both count as overlaps) does not ensure its satisfaction after we have specified a distinct assignment, so we must place another overlap condition on the inner sum. We may eliminate A from the condition on C, by noting that A is a function (call it $\mathfrak{a}$) of C,

$$A = \mathfrak{a}(C) \quad . \tag{A4}$$

Schematically, $\mathfrak{a}(C) = B_1 \cdots B_n F/\mathcal{K}_\alpha$. Then we need require of C only that $\mathcal{K}_\alpha$ be contained in $B_1 \cdots B_n F$ (and B_i overlaps $\mathcal{K}_\alpha$, as before) if we insert a Kronecker delta function $\delta_{A,\mathfrak{a}(C)}$. We now divide the C's into equivalence classes under G [where

$g \in G$ acts on C by rotating all the operators in (A2) simultaneously]. We pick a distinguished member $\bar{C}$ of each equivalence class (in practice, this is the first member in a dictionary ordering of C's induced by the ordering of the B's). Our sum over C's may now be written as a sum over P's [Eq. (A1)], then over $\bar{C}$'s, and finally over $C = g\bar{C}$ in the equivalence class of $\bar{C}$. So (A3) becomes

$$\frac{d(A)}{d\beta} = -\sum_P \gamma_{\bar{\alpha}}(\bar{B}_1)\cdots(\bar{B}_n) \times \sum_{\bar{C}:\ \text{each } B_i \text{ overlaps } \mathcal{K}_\alpha,\ \mathcal{K}_\alpha \text{ in } B_1\cdots B_n F} \times \sum_{C(=g\bar{C})} \delta_{A,\mathfrak{a}(C)} \sum_{\text{d.a. (each } B_i \text{ overlaps } \mathcal{K}_\alpha)} \sigma_{\text{d.a.}} \quad . \tag{A5}$$

We have taken advantage of the facts that $\gamma_\alpha(B_1)\times\cdots(B_n)$ depends only upon P, and that the conditions on the C sum are invariant under G (so we need only check them for $\bar{C}$). Noting that the innermost sum (over distinct assignments) is invariant under G, we may write it as a function f_a of $\bar{C}$ (the "assignment factor")

$$f_a(\bar{C}) = \sum_{\text{d.a. (each } B_i \text{ overlaps } \mathcal{K}_\alpha)} \sigma_{\text{d.a.}} \quad . \tag{A6}$$

Since we are interested only in calculating one cumulant from each equivalence class, we replace A by $\bar{A}$ in (A5), giving

$$\frac{d(\bar{A})}{d\beta} = \sum_P \gamma_{\bar{\alpha}}(\bar{B}_1)\cdots(\bar{B}_n) \times \sum_{\bar{C}:\ \text{each } B_i \text{ overlaps } \mathcal{K}_\chi,\ \mathcal{K}_\alpha \text{ in } B_1\cdots B_n F} \times f_a(\bar{C}) \sum_{C(=g\bar{C})} \delta_{\bar{A},\mathfrak{a}(C)} \quad . \tag{A7}$$

We observe that $\mathfrak{a}(C) = \mathfrak{a}(g\bar{C}) = g\mathfrak{a}(\bar{C})$, so that the sum over C in (A7) vanishes unless $\mathfrak{a}(\bar{C})$ is in the equivalence class of $\bar{A}$, i.e., $\bar{A} = \bar{\mathfrak{a}}(\bar{C})$. The sum may therefore be replaced by

$$\delta_{A,\bar{\mathfrak{a}}(\bar{C})} f_s(\bar{C}) \quad ,$$

where

$$f_s(\bar{C}) = \sum_{C(=g\bar{C})} \delta_{\bar{\mathfrak{a}}(\bar{C}),g\mathfrak{a}(\bar{C})} \tag{A8}$$

is the "symmetry factor." It simply counts the distinct rotations of $\bar{C}$ which leave $\mathfrak{a}(\bar{C})$ fixed. (If the F in $\bar{C}$ has more than zero pairs, we must omit operations g involving Hermitian conjugation.)

Our final result is

$$\frac{d(\bar{A})}{d\beta} = -\sum_P \gamma_{\bar{\alpha}}(\bar{B}_1)\cdots(\bar{B}_n) \times \sum_{\bar{C}:\ \text{each } B_i \text{ overlaps } \mathcal{K}_\alpha, \mathcal{K}_\alpha \text{ cont. in } B_1\cdots B_n F} \times f_a(\bar{C}) f_s(\bar{C})\ \delta_{\bar{A},\bar{\mathfrak{a}}(\bar{C})} \quad , \tag{A9}$$

where f_a, f_s, and $\mathfrak{a}$ are defined by (A6), (A8), and (A4). P was defined by (A1), and the $\bar{C}$ are inequivalent configurations of the form (A2).

Equation (A9) is the basis of our automatic algorithm. For each product of cumulants (i.e., P) satisfying (17), we generate all possible $\bar{C}$'s (since we may leave $\mathcal{K}_{\bar{\alpha}}$ fixed, and each B_i must overlap $\mathcal{K}_{\bar{\alpha}}$, there are clearly a finite number of $\bar{C}$'s). For each $\bar{C}$ we compute f_a, f_s, and $\bar{A} = \bar{\mathfrak{a}}(\bar{C})$. We determine an integer label L for $\bar{A}$ by finding $\bar{A}$ in our list of cumulants (or adding it at the end, if it is not there). For each product P, we store a number of pairs $(L, f_a f_s)$, one for each $\bar{C}$. (For several selected P's, we give all the resulting pairs in Table III. Each row in the first two columns specifies a P; the last two columns give L and $f_a f_s$, respectively, one row per pair.) This information is used every time we iterate the differential equations; it determines how to increment the cumulants.

---

*Research supported in part by the National Science Foundation under Grant No. GH 33634.

†Present address: Dept. of Physics, University of California, San Diego, La Jolla, Calif. 92037.

[1]J. Hubbard, Proc. R. Soc. A 276, 238 (1963).

[2]H. Shiba and P. A. Pincus, Phys. Rev. B 5, 1966 (1972); D. Cabib and T. A. Kaplan, *ibid.* 7, 2199 (1973); K. H. Heinig and J. Monecke, Phys. Status Solidi B 49, K139 (1972).

[3]R. A. Bari and T. A. Kaplan, Phys. Rev. B 6, 4623 (1972).

[4]W. Langer, M. Plischke, and D. Mattis, Phys. Rev. Lett. 23, 1448 (1969), among others.

[5]Some other approximations have correctly predicted a smooth transition. See, for example, T. A. Kaplan and R. A. Bari, J. Appl. Phys. 41, 875 (1970); J. C. Kimball and J. R. Schrieffer, in *Magnetism in Alloys*, edited by P. A. Beck and J. T. Waber (Am. Inst. of Mining, Metallurgical and Petroleum Engineers, Boston, Mass., 1972).

[6]Bari and Kaplan (Ref. 3) have pointed out that the high-temperature state (which is not degenerate) cannot properly be called a metal.

[7]P. B. Visscher, following paper, Phys. Rev. B 10, 943 (1974).

[8]Extension of Hubbard's equations (Ref. 1) to higher order is very difficult because his equations for higher-order Green's functions involve the equal-time expectation values, which are not known *a priori*. Since the present technique remedies this at high temperature, an exact numerical version of the Hubbard calculation may be possible, enabling the calculation of nonequilibrium properties (time-dependent Green's functions).

[9]K. Huang, *Statistical Mechanics* (Wiley, New York, 1963).

[10]We assume here that γ_α is independent of β. In practice we would like to fix $\langle n \rangle$, which requires μ to vary with β. It is easily seen that if γ_α depends on β, it

should be replaced in Eq. (6) by $\gamma'_\alpha = d(\beta\gamma_\alpha)/d\beta$. Then $\mu'(\beta)$ may be determined from the requirement $d\langle n\rangle/d\beta = 0$.

[11]We could alternatively differentiate with respect to any of the γ_α which multiplies an operator which commutes with the rest of the Hamiltonian, e.g., chemical potential or magnetic field. We would then obtain an equation for following the system as the density is changed or a field is applied.

[12]Reference 9, p. 305.

[13]It should be made clear that we are invoking the Hartree-Fock approximation only to motivate an exact transformation of exact equations. Our results in no way depend upon the validity of the Hartree-Fock approximation, which can give very misleading results for the Hubbard model (see Sec. I).

[14]For the Hubbard Hamiltonian (or any other involving only two-body interactions) we have $n \leq 4$. This is because each $B_i (i = 1, \cdots n)$ must share with $\mathcal{H}_\alpha$ a $c^\dagger$ or a c, of which $\mathcal{H}_\alpha$ has at most 4.

[15]We must also input the integration interval $\Delta\beta$. But good convergence with respect to $\Delta\beta$ is easy to achieve [and we could make it even easier by using a Runge-Kutta technique instead of Eq. (16)] so we make no more mention of it.

[16]M. Ferer and M. Wortis, Phys. Rev. B 6, 3426 (1972); M. Ferer, Ph. D. thesis (University of Illinois, 1972) (unpublished).

[17]J. Bonner and M. Fisher, Phys. Rev. 135, A 640 (1964).

[18]Our result for the transition temperature is much higher than the value found by A. J. Epstein, S. Etemad, A. F. Garito, and A. J. Heeger [Phys. Rev. B 5, 952 (1972)] in their experiments on charge-transfer salts (if we adopt their value for the intra-atomic repulsion). It has been suggested that these materials might behave as the one-dimensional Hubbard model; the implications of the transition-temperature inconsistency for this hope are discussed in Ref. 3.

[19]Numerical uncertainties in $\langle n_\uparrow n_\downarrow \rangle$ are much smaller than in the specific heat. Error bars are omitted because they would not be resolvable in the figures; the largest uncertainty in $\langle n_\uparrow n_\downarrow \rangle$ (about 5%) is in Fig. 4(a).

[20]E. H. Lieb and F. Y. Wu, Phys. Rev. Lett. 20, 1445 (1968).

[21]Shiba and Pincus obtain a nonmonotonic $\langle n_\uparrow n_\downarrow \rangle$ with a dip at $\beta \approx 1.2$ (their $L_0 = \frac{3}{4} - \frac{3}{2}\langle n_\uparrow n_\downarrow \rangle$). Figure 4(a) shows that this is probably a size effect (they use a six-atom ring).

[22]G. A. Baker, H. E. Gilbert, J. Eve, and G. S. Rushbrooke, Phys. Lett. 20, 146 (1966).

[23]Y. Nagaoka, Phys. Rev. 147, 392 (1966).